IEEE Access
Multidisciplinary | Rapid Review | Open Access Journal

Received 11 September 2023, accepted 1 October 2023, date of publication 10 October 2023, date of current version 18 October 2023.

Digital Object Identifier 10.1109/ACCESS.2023.3323251

RESEARCH ARTICLE

Analysis of the Propagation Characteristics of Acoustic Waves From Leakages in Buried Gas Pipelines

SONG LIU[1,2], ANQI LIU[3], ZEFENG CAI[4], CHUNFENG SUN[1,2], AND RUOCHEN LIU[1,2]

[1]Hebei Key Laboratory of Hazardous Chemicals Safety and Control Technology, Beijing 101601, China
[2]School of Chemical Safety, North China Institute of Science and Technology, Beijing 101601, China
[3]CNPC Research Institute of Safety and Environment Technology, Beijing 102206, China
[4]Beijing Haifurun Technology Company Ltd., Beijing 100102, China

Corresponding author: Ruochen Liu (ruochen.liu@ncist.edu.cn)

This work was supported by the Fundamental Research Funds for the Central Universities under Grant 3142023026.

ABSTRACT In order to accurately detect the leakages in buried gas pipelines and to reduce the leakage amount and false alarms, the propagation characteristics of acoustic waves owing to leakages in buried gas pipelines are analyzed. Firstly, the coupling effect of soil particles and gas, including the diffusion of acoustic waves by the soil, the scattering of acoustic waves by particles in the soil and the absorption of acoustic energy by the soil medium, is considered to establish a propagation attenuation model for acoustic waves resulted from leakages in buried gas pipelines. As acoustic waves are prone to the influence of noise in the process of propagation, an improved extreme-point symmetric mode decomposition (IESMD) acoustic signal denoising algorithm is proposed, which can effectively filter out the noise in the signal. The experimental results prove the accuracy and denoising capability of the established acoustic wave attenuation model for buried gas pipelines, demonstrating a potential improvement of the leakage detection technology for buried pipelines.

INDEX TERMS ESMD, acoustic waves, attenuation model, leak detection, buried gas pipeline.

I. INTRODUCTION

The transmission pipelines of gas and other energy sources are mainly buried underground, often leading to leakages due to ageing pipes, rainwater corrosion and many other reasons [1], [2]. A buried gas pipeline leakage could result in not only pollution to the soil along the pipeline, but also waste of natural gas and other energy, and may even cause accidents and jeopardize people's lives and health [3]. Therefore, it is of great significance to analyze the propagation characteristics of buried pipeline leakage signals to achieve the accuracy of pipeline leakage detection.

Currently, in the field of pipeline leakage detection, various types of detection techniques are emerging with the development of technology, which could be divided into hardware-based and software-based detection methods [4], [5]. Hardware-based detection methods include infrared sensor detection, fiber optic sensor detection [6], [7] and pipeline robot detection. Software-based detection methods include negative pressure wave detection [8], [9], neural network detection [10], and acoustic wave detection [11]. Hardware-based detection methods such as infrared sensor detection have many shortcomings such as high cost of use and maintenance problems [12]. The software-based detection method, represented by the acoustic method, has the advantages of low cost and simple maintenance [13]. In particular, the acoustic wave detection method could achieve real-time signal detection with outstanding performance in the detection speed and detection accuracy, while acoustic waves of leakages in the process of propagation is prone to the influence of environmental and equipment noise [14]. Therefore, how to effectively filter out the noise information in the

The associate editor coordinating the review of this manuscript and approving it for publication was Md. Kamrul Hasan.

acoustic wave is very important. Meng et al. improved the ensemble empirical mode decomposition (EEMD) denoising algorithm that could effectively filter the noise in the acoustic signal based on the shortcomings of the algorithm via mutual spectrum analysis [15]. Li et al. proposed a complete ensemble empirical mode decomposition with adaptive noise (CEEMDAN) denoising algorithm based on independent volume analysis optimization, of which the result showed that the optimized algorithm could select the eigenmode components that contain more useful information, and the reconstructed signal had lower noise content [16].

For the studies to the propagation characteristics of leaking acoustic waves, Lang et al. investigated the generation mechanism of fluid pipeline leaks according to the method of feature theory and analyzed the wave velocity propagation of ultrasonic waves to establish a calculation model for the attenuation of ultrasonic signals in fluid pipelines [9]. Liu et al. modified the existing research of the acoustic waves propagation model of oil and gas pipes so that a new computational model was developed by analyzing the effects of damping that caused attenuation [17]. Sun constructed a mathematical model for leaking pipes based on the circuit as an inspiration and treated the flow characteristics at the end of the pipe with experimentally verified good performance [18].

In order to accurately detect leaks in buried gas pipelines and reduce leakage and false alarms in the detection system, this paper analyses the propagation characteristics of leaky acoustic waves in buried gas pipelines. When a leakage occurs in a buried gas pipeline, the soil around the pipeline will be deformed internally, and the soil particles are coupled with the gas around, generating an interference signal that affects the attenuation model of the leakage acoustic wave. Based on the environment in which the buried pipeline is laid, this paper considers the coupling effect of soil particles and gas, and establishes an attenuation model for the propagation of acoustic waves from buried gas pipeline leaks. ESMD [19], [20] is an effective denoising algorithm, but its performance would be influenced by the impulse signals and noise during the decomposition process, resulting in multiple changes in the extreme points of the curve in a short period of time. To effectively filter out noise and impulse signals and retain useful information related to the leakage, this paper proposes an acoustic signal denoising algorithm with improved ESMD, verified by the experiments to demonstrate the denoising performance of the algorithm.

II. LEAKAGE ACOUSTIC ATTENUATION MODEL FOR OVERBURDEN CONDITIONS

When a leakage occurs in a buried gas pipeline, due to the internal deformation of the soil and the coupling of soil particles with the gas, interference signals of different frequencies, amplitudes and energy characteristics are generated, which in turn affects the attenuation model of the leakage acoustic wave [21], [22]. It is proposed to introduce dynamic attenuation components in the environment on the basis of the acoustic wave attenuation model, and to fully consider the diffusion of acoustic waves by the soil, the scattering of acoustic waves by particles in the soil and the absorption of acoustic energy by the soil medium, to design an effective model for the attenuation of leaky acoustic waves of buried gas pipelines under overburden conditions.

The equation for the fluctuation of an acoustic wave in an ideal medium in a pipe is as follows [23]:

$$\frac{\partial^2 p}{\partial x^2} = \frac{1}{c_0^2}\frac{\partial^2 p}{\partial t^2} \tag{1}$$

where p is the acoustic wave amplitude, c_0 is the speed of acoustic in air, t is time and x is the axial distance, respectively.

According to the energy propagation loss process, the acoustic wave amplitude propagation at the leakage point decays along the pipeline in an approximate exponential form, and the mathematical model for its decay is as follows [24]:

$$|\Delta p_x| = |\Delta p_0|\, e^{-\lambda x} \tag{2}$$

where, $|\Delta p_0|$ is the acoustic wave amplitude at the end of the pipe, Δp_x is the acoustic wave amplitude at the distance x from the leak, and λ is the acoustic attenuation coefficient.

$$\lambda = \frac{1}{r c_v}\sqrt{\frac{\pi f}{\rho_0}}\sqrt{\theta} \tag{3}$$

where, r is the diameter of the pipe, c_v is the speed of acoustic propagation, f is the frequency of the acoustic wave, ρ_0 is the density of the medium and θ is the coefficient of viscosity.

The acoustic wave attenuation coefficient in the acoustic wave attenuation model of (2) does not consider the coupling effect of soil particles and gases, including the diffusion of acoustic waves by the soil, the scattering of acoustic waves by particles in the soil and the absorption of acoustic energy by the soil medium. In this paper, according to the actual situation of the buried pipeline site, the above factors are taken into account, and (2) is improved so that it can accurately describe the acoustic wave attenuation of buried pipelines. The scattering attenuation coefficient of acoustic waves in the soil is defined as λ_1, the absorption attenuation coefficient of acoustic waves in the soil is λ_2, and other factors such as dispersion attenuation, adjacent media interference are simplified to λ_3. In turn, the effect of the soil environment on the acoustic signal of a pipeline leak is analyzed.

Since the values of $\lambda_1, \lambda_2, \lambda_3$ are not fixed, the exact values need to be determined according to the site environment. In this paper, a comprehensive analysis of the above influencing factors is carried out based on the previous related studies [25], [26], [27] to define the attenuation coefficient κ of acoustic waves in the buried environment ($\kappa = \lambda \cdot \lambda_1 \cdot \lambda_2 \cdot \lambda_3$) with proper verifications and adjustments according to the conditions of experiment site. The buried pipeline micro-leakage acoustic attenuation model is then established

with the mathematical description as follows:

$$|\Delta p_x| = |\Delta p_0| \, e^{-\kappa x} \tag{4}$$

The buried pipeline leakage acoustic attenuation model established in this paper fully takes the influence of the soil environment on the acoustic signal into account and can more effectively describe the acoustic propagation characteristics of pipeline leakage under overburden conditions. Fig. 1 shows the principle of establishing the acoustic attenuation model for pipeline leakage under overburden conditions.

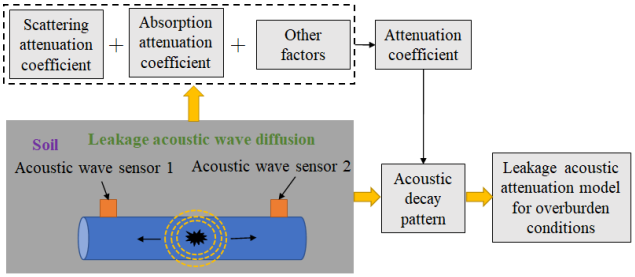

FIGURE 1. Principles for modelling acoustic wave attenuation of leakage under overburden conditions.

III. DENOISING OF ACOUSTIC SIGNALS FROM BURIED PIPELINE LEAKS

A. EXTREME-POINT SYMMETRIC MODE DECOMPOSITION

ESMD is an improvement on empirical mode decomposition (EMD), which not only retains the advantages of EMD but also demonstrates capabilities to overcome the shortcomings of EMD (e.g., modal mixing) with good decomposition performance. Its decomposition steps are as follows [19], [28], [29]:

(1) Define the signal to be decomposed as $X(t)$, determine the individual extreme and minima of the signal, each of which is denoted as $E_i = (x_i, y_i), i = 1, 2, \cdots, n$, where x_i and y_i are the horizontal and vertical coordinates of the extreme points, respectively. Connect all the extrema and take the midpoint between adjacent extrema defined as Z_i by (5), and then find the boundary points at both ends of the line segment and define them as Z_0 and Z_m.

$$Z_i = (\frac{x_i + x_{i+1}}{2}, \frac{y_i + y_{i+1}}{2}) \tag{5}$$

(2) Interpolate the midpoints and boundary points defined in step (1) to obtain m interpolation curves $J_1, J_2, \cdots J_m$. The mean curve J^* of the curves is then calculated by (6).

$$J^* = \frac{(J_1 + J_2 + \cdots + J_m)}{m} \tag{6}$$

(3) Use $X(t)$-J^* as the input to the system, repeat steps (1)-(2) until $|J^*| < \varphi$ (φ is the allowed error threshold) or the number of screenings has reached S, then stop the loop execution. At this point, the first modal component IMF1 can be obtained.

(4) Use $X(t)$-IMF1 as a new input source signal and repeat steps (1)-(3) until all IMFs are obtained from the decomposition. Stop the loop when the number of extreme points does not satisfy the requirement. The function obtained at this point is called the optimal AGM curve $Q(t)$.

(5) Set the value interval of the maximum number of screening times S to $[S_{\min}, S_{\max}]$, take the value of S in this interval, and then repeat the above process. At the same time, calculate the standard deviation λ of $X(t)$-$Q(t)$ and the standard deviation λ_0 of the signal $X(t)$. At this time, we can get the trend of the variance ratio λ/λ_0 and the number of screening times S. The number of screening times S obtained when the variance ratio is smallest is the optimal number of screening times S_0.

(6) Make $S = S_0$ and repeat steps (1)-(4) to obtain the final IMF and residual components $r_k(t)$ as shown in (7).

$$X(t) = \sum_{i=1}^{k} IMF_i + r_k(t) \tag{7}$$

B. IMPROVED ESMD

In the ESMD decomposition algorithm, the first step is to locate all the extreme points of the source signal, which are then connected to select the midpoint between two adjacent extreme points, and by connecting each midpoint the mean curve could be obtained. The signal is often affected by noise, impulse signals and other factors, and the extreme points of the curve may change several times in a short period of time. Therefore, the distribution and selection of the extreme value points of the curve can have a great impact on the performance of the decomposition algorithm. To address the above problems, the ESMD algorithm is improved in this paper as following steps:

(1) For the signal $X(t)$, we let $e_0(t) = X(t), f_l(t) = e_i(t)$, $l = 1, i = 1$.

(2) Determine all the extreme and minimal value points of $f_{l-1}(t)$ and write $(\sigma_n^l, X_n^l), n = 1, 2, \ldots, N$, where σ_n^l and X_n^l are the values of the horizontal and vertical coordinates of each extreme point, respectively, at which point defines the new extreme value point:

$$Q_n^l = \frac{X_{n-1}^l + \partial X_n^l + X_{n+1}^l}{2 + \partial}, \quad n = 2, 3 \cdot \cdot, N - 1 \tag{8}$$

where ∂ is weighting factor. In this paper, the values of ∂ are taken in the range of 1.5 to 2.3 with one decimal place and substituted into (5) to screen the value with the best results.

(3) The new extreme point can be obtained by end-point extension as (σ_n^l, Q_n^l), where σ_n^l and Q_n^l are the values of the horizontal and vertical coordinates of each new extreme point, respectively, and then two adjacent new

extreme points are connected to obtain the midpoint Z_i' of the two new extreme points by (9). Define the boundary points at the ends of the line segment as Z_0' and Z_m'.

$$Z_i' = \left(\frac{x_i' + x_{i+1}'}{2}, \frac{y_i' + y_{i+1}'}{2}\right) \tag{9}$$

(4) Interpolate the midpoints and boundary points defined in step (3) to obtain m interpolation curves $J_1', J_2', \cdots J_m'$. The mean curve J' of the curves is then calculated by (10).

$$J' = \frac{(J_1' + J_2' + \cdots + J_m')}{m} \tag{10}$$

(5) Using $X(t) - J'$ as inputs to the system, repeat steps (3)-(4) until $|J'| < \varphi$ or the number of screenings reaches S', then stop the loop execution. At this point, the first modal component IMF1 could be obtained.

(6) Using $X(t)$-IMF1 as a new input source signal, repeat steps (1)-(5) to obtain all IMFs. Stop the loop when the number of extreme points does not satisfy the requirement. The function obtained at this point is called the optimal AGM curve $Q'(t)$.

(7) Set the value interval of the maximum number of screening times S' to $[S'_{\min}, S'_{\max}]$, take the value of S' in this interval, and then repeat the above process. At the same time, calculate the standard deviation η of $X(t) - Q'(t)$ and the standard deviation η' of the signal X(t). At this time, the trend of the variance ratio η/η' and the number of screening times S' could be calculated. The number of screening times S' obtained is the optimal number of screening times S_0' when the variance ratio is smallest. Repeat step (1)-(6) to obtain the final IMF and residual components $R_k(t)$ as shown in (11).

$$X(t) = \sum_{i=1}^{k} IMF_i + R_k(t) \tag{11}$$

IV. EXPERIMENT AND DISCUSSION

For verification and validation of the theory in this paper, an experimental analysis was carried out on a buried gas pipeline of a gas company and the experimental site is shown in Fig. 2. The length of the buried pipe used in the experiment was 3000 m with a pipe diameter of 200 mm and the pipe was 1.2 m underground. Leakage ball valves were installed at 500 m, 1300 m, 2000 m and 2700 m of the buried pipeline, with pressures of 2.2 MPa and 0.8 MPa at the beginning and end respectively. The leakage ball valves were available in 6 mm, 8 mm and 10 mm to simulate the leakage under different conditions. The acoustic sensor adopted in the experiments was a high sensitivity ICP 106B acoustic sensor. The data collector was an 8-channel synchronous data collector, which was controlled by a program written in LabVIEW software and the sampling frequency was set to 1000 Hz. The experimental schematic is shown in Fig. 3.

FIGURE 2. Site photo of buried gas pipeline leakage experiment for theory verification and validation.

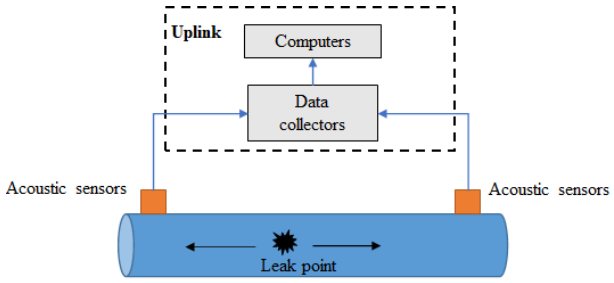

FIGURE 3. Schematic of buried gas pipeline leakage experiment for theory verification and validation.

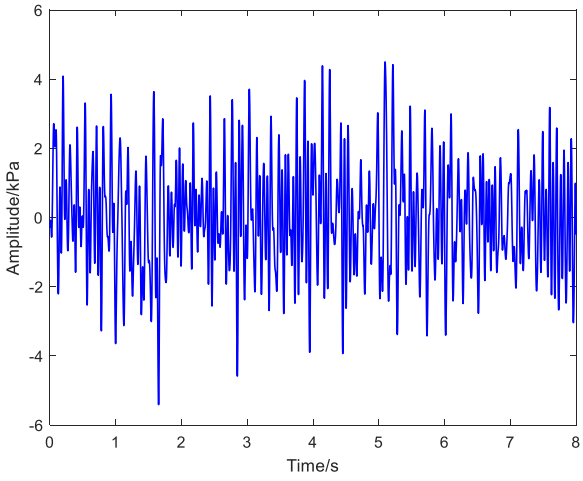

FIGURE 4. Acoustic signal curve collected by the acoustic sensors from buried gas pipeline leakage experiments.

A. ANALYSIS OF DENOISING PERFORMANCE

The acoustic signal collected by the acoustic sensor at the first end of the pipeline was used as an example to denoise the signal. The signal curve collected by the acoustic sensor at the first end of the pipeline when the 6 mm ball valve at 1300 m in the buried pipeline was opened is shown in Fig. 4. As can be seen from Fig. 4, the acoustic signal curve

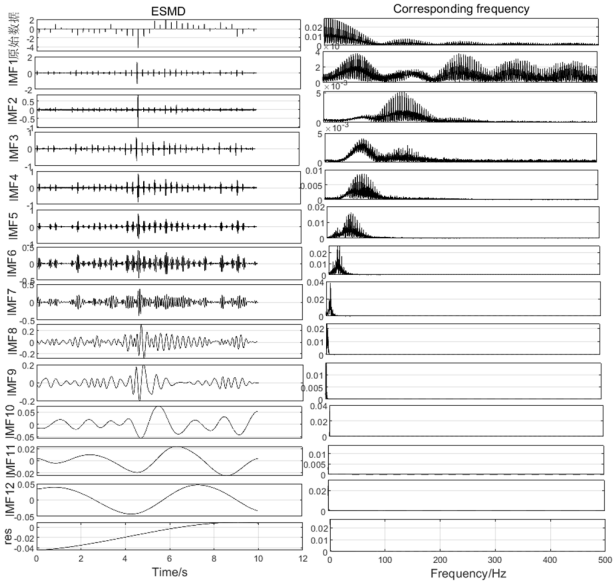

FIGURE 5. Each IMF component and its spectrum decomposed by IESMD decomposition algorithm.

collected by the acoustic sensor contains a large amount of noise and other disturbing information without processing, resulting in the fluctuating and disorganized signal curve which prevent the leakage in the buried pipeline from being accurately located. The IESMD decomposition algorithm was used to decompose the acquired acoustic signal curve, and the decomposed IMF components and their spectra were obtained as shown in Fig. 5. It should be noted that the best result was obtained when the value of ∂ was taken as 2 after a number of experimental tests, which revealed an interesting future research topic to the determination of optimal value of ∂ by an efficient method.

The IESMD decomposition yielded 12 IMF components and one residual component. The IMF components were reconstructed to obtain the acoustic signal profile after denoising. Under the same conditions, the EMD and ESMD decomposition algorithms were used to denoise the acquired signal profiles. A comparison of the EMD, ESMD and IESMD profiles is shown in Fig. 6.

Although the performance of each denoising method can be clearly distinguished from the signal curves in Fig. 6, there are certain criteria for judging the performance of denoising. To compare the denoising performance of different denoising algorithms, this paper uses Root Mean Square Error (RMSE) and Signal-to-Noise Ratio (SNR) to compare and evaluate the performance of each denoising algorithm. In order to evaluate the performance of the denoising methods proposed in this paper, EMD, ESMD, ESMD-WSST [30] and MF-ESMD [31] are introduced to compare with the denoising method in this paper and to evaluate the performance of the proposed method. The comparison results are shown in Table 1.

Table 1 shows that the RMSE values for the EMD, ESMD, ESMD-WSST, and MF-ESMD methods are 0.0822, 0.0694, 0.0341, and 0.0305, and the SNR values are 21.760,

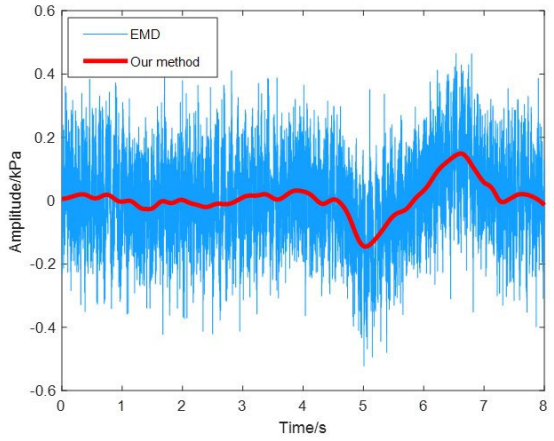

(a) Comparison of EMD and our proposed method

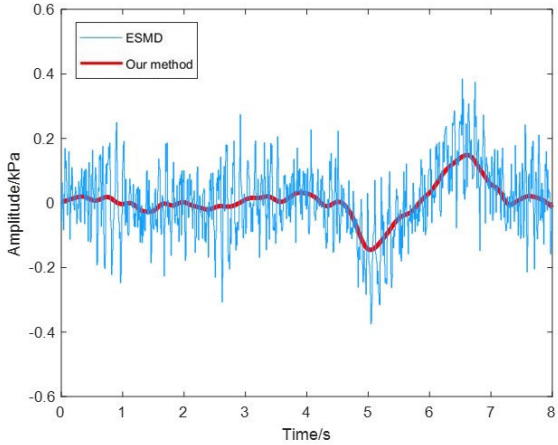

(b) Comparison of ESMD and our proposed method

FIGURE 6. Performance comparisons of acoustic signal profiles generated by different denoising methods.

TABLE 1. Performance comparisons of different denoising methods.

	EMD	ESMD	ESMD-WSST	MF-ESMD	IESMD
RMSE	0.0822	0.0694	0.0341	0.0305	0.0263
SNR	21.760	24.022	25.409	24.929	25.791

24.022, 25.409, and 24.929, respectively, while the values of RMSE and SNR of the denoising algorithm for IESMD are 0.0263 and 25.791, respectively. As shown in the comparison, the RMSE of IESMD is significantly lower than other methods and the SNR is significantly higher than the values of other methods. For a signal, a smaller value of MSE and a larger value of SNR indicate a better quality of the signal. Therefore, the proposed denoising algorithm is significantly better than the other algorithms and could effectively filter out noise and other disturbing information from the signal.

B. PERFORMANCE ANALYSIS OF THE ATTENUATION CALCULATION MODEL

The 6 mm, 8 mm and 10 mm ball valves were operated at 500 m, 1300 m, 2000 m and 2700 m of the buried gas pipeline respectively to simulate leakage at different locations in the pipeline with different leakage orifice sizes. The signals

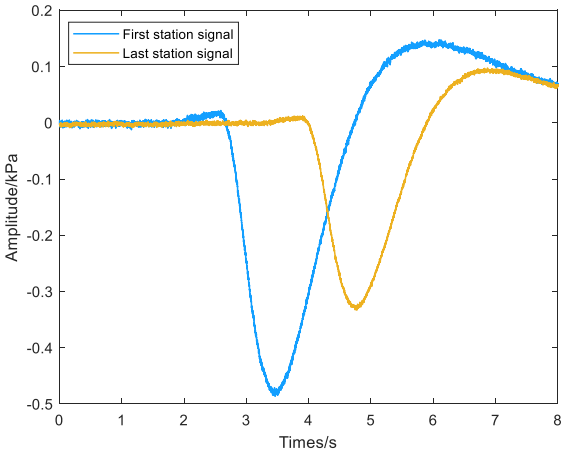

FIGURE 7. Leakage signal curve when 6 mm ball valve was opened at 500 m of pipeline.

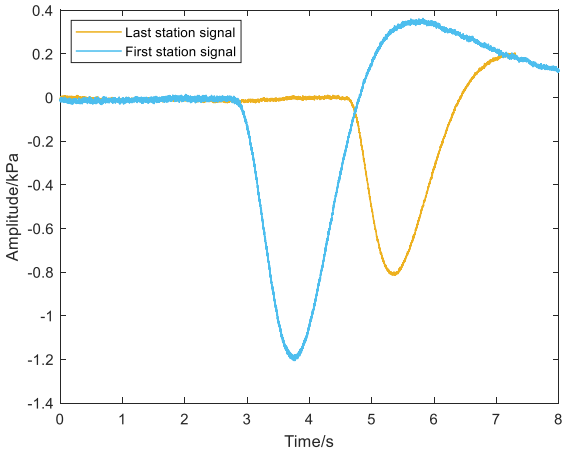

FIGURE 8. Leakage signal curve when 8 mm ball valve was opened at 500 m of pipeline.

collected by the first end acoustic sensors were then denoised using the IESMD method ($\partial = 2$). Fig. 7 to Fig. 9 show the signal curves taken at 500 m of the pipeline under different conditions of leakage. The blue curve in the figure is the signal curve after denoising at the first station of the pipeline, and the yellow curve is the signal curve after denoising at the end station of the pipeline. As can be seen from these figures, the noise has been basically filtered out by the IESMD algorithm denoising process so that the inflection point of the signal can be determined very accurately from the smoothed signal curve. At this point, the measured values of acoustic wave amplitude at the first and last stations of the pipeline could be derived from the figure, which is then substituted into (4) to obtain the calculated value of the acoustic wave amplitude at the first station of the pipeline. According to Fig. 7 - Fig. 9, when 6mm, 8mm and 10mm leakage occurs at 500 m, the measured acoustic wave amplitudes at the first station of the pipeline are 0.473 kPa, 1.196 kPa and 3.113 kPa, and at the last station, the measured acoustic wave amplitudes are 0.365 kPa, 0.861 kPa and 1.726 kPa, respectively. The measured acoustic amplitudes of the first and last station under other operating conditions could also be obtained by this method. The value of acoustic attenuation coefficient λ is set to 0.11 based on the field environment. As shown in Table 2, the calculated value of the amplitude of the acoustic wave at the first station is compared with the measured value in the field to demonstrate the accuracy performance of the established model in this paper. In Table 2, $|\Delta p_0|$ and $|\Delta p_x|$ are the amplitudes of the acoustic signals measured at the last and first station, which could be obtained by denoising the acoustic signal collected at the site. The calculated value of $|\Delta p_x|$ is calculated according to (4).

Table 2 shows the calculated value of the acoustic wave amplitude obtained from the acoustic wave amplitude calculation model established in this paper is almost equal to the amplitude obtained from the actual measurement in the field for various sizes and locations of the pipeline leakages with negligible errors. The results demonstrate that the acoustic wave amplitude calculation model established in this paper can accurately calculate the amplitude of acoustic waves for the buried pipeline leakages with arbitrary sizes and locations, indicating the application of this method to effectively improve the detectability of buried pipeline leakages.

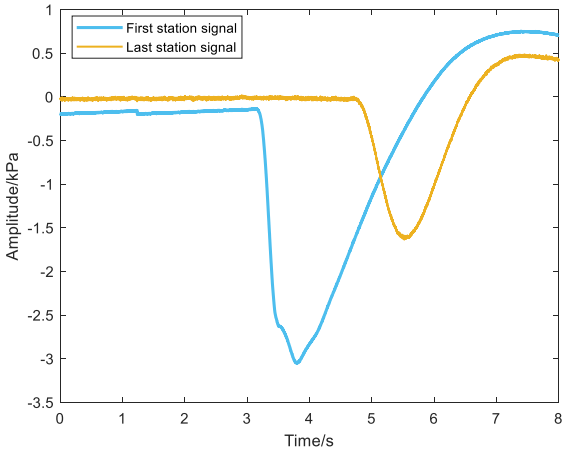

FIGURE 9. Leakage signal curve when 10 mm ball valve was opened at 500 m of pipeline.

TABLE 2. Comparison between measured and calculated values of leakage sound wave attenuation.

Location of the leak	Leak hole diameter	$\lvert\Delta p_0\rvert$ /kPa	$\lvert\Delta p_x\rvert$ /kPa	Calculated value of $\lvert\Delta p_x\rvert$ /kPa
500 m	6 mm	0.365	0.473	0.468
	8 mm	0.861	1.196	1.199
	10 mm	1.726	3.113	3.120
1300 m	6 mm	0.253	0.179	0.183
	8 mm	1.231	1.068	1.074
	10 mm	3.069	2.882	2.796
2000 m	6 mm	0.219	0.155	0.157
	8 mm	1.081	0.964	0.959
	10 mm	2.966	2.636	2.631
2700 m	6 mm	0.177	0.136	0.133
	8 mm	1.011	0.838	0.843
	10 mm	2.659	2.218	2.211

V. CONCLUSION

This paper proposed a new method to detect leakages at the buried gas pipelines in a timely and accurate manner. The diffusion of acoustic waves by the soil, the scattering of acoustic waves by particles in the soil and the absorption of acoustic energy by the soil medium are first analyzed to obtain the acoustic wave propagation characteristics of the buried gas pipelines leakages. A calculation model for acoustic wave propagation attenuation of buried pipelines is then established. In addition, the present work optimizes the ESMD denoising method to improve existing shortcomings to further reduce the disturbances of the acoustic signal, resulting in a relatively low noise level in the acoustic signal. Finally, field experiments were carried out to illustrate the performance of the model established in this paper with good accuracy and denoising capability, demonstrating a potential improvement of the leakage detection technology for buried pipelines.

REFERENCES

[1] L. Mei, J. Zhou, S. Li, M. Cai, and T. Li, "Leak identification based on CS-ResNet under different leakage apertures for water-supply pipeline," *IEEE Access*, vol. 10, pp. 57783–57795, 2022.

[2] K. Sitaropoulos, S. Salamone, and L. Sela, "Frequency-based leak signature investigation using acoustic sensors in urban water distribution networks," *Adv. Eng. Informat.*, vol. 55, Jan. 2023, Art. no. 101905.

[3] J. Wang, L. Zhao, T. Liu, Z. Li, T. Sun, and K. T. V. Grattan, "Novel negative pressure wave-based pipeline leak detection system using fiber Bragg grating-based pressure sensors," *J. Lightw. Technol.*, vol. 35, no. 16, pp. 3366–3373, Aug. 15, 2017.

[4] A. Cataldo, G. Cannazza, E. De Benedetto, and N. Giaquinto, "A new method for detecting leaks in underground water pipelines," *IEEE Sensors J.*, vol. 12, no. 6, pp. 1660–1667, Jun. 2012.

[5] S. M. Mujtaba, T. A. Lemma, S. A. A. Taqvi, T. N. Ofei, and S. K. Vandrangi, "Leak detection in gas mixture pipelines under transient conditions using Hammerstein model and adaptive thresholds," *Processes*, vol. 8, no. 4, p. 474, Apr. 2020.

[6] J. Zuo, Y. Zhang, H. Xu, X. Zhu, Z. Zhao, X. Wei, and X. Wang, "Pipeline leak detection technology based on distributed optical fiber acoustic sensing system," *IEEE Access*, vol. 8, pp. 30789–30796, 2020.

[7] Y. Xu, J. Li, M. Zhang, T. Yu, B. Yan, X. Zhou, F. Yu, J. Zhang, L. Qiao, T. Wang, and S. Gao, "Pipeline leak detection using Raman distributed fiber sensor with dynamic threshold identification method," *IEEE Sensors J.*, vol. 20, no. 14, pp. 7870–7877, Jul. 2020.

[8] L. Yang and Q. Zhao, "A BiLSTM based pipeline leak detection and disturbance assisted localization method," *IEEE Sensors J.*, vol. 22, no. 1, pp. 611–620, Jan. 2022.

[9] J. Wang, L. Ren, Z. Jia, T. Jiang, and G.-X. Wang, "A novel pipeline leak detection and localization method based on the FBG pipe-fixture sensor array and compressed sensing theory," *Mech. Syst. Signal Process.*, vol. 169, Apr. 2022, Art. no. 108669.

[10] X. Lang, P. Li, J. Cao, Y. Li, and H. Ren, "A small leak localization method for oil pipelines based on information fusion," *IEEE Sensors J.*, vol. 18, no. 15, pp. 6115–6122, Aug. 2018.

[11] Y. Zhu, X. Lang, L. Zhang, and Z. Cai, "Leak localization method of jet fuel pipeline based on second-generation wavelet transform and short-time energy time delay estimation," *IEEE Sensors J.*, vol. 23, no. 3, pp. 2823–2832, Feb. 2023.

[12] X. Hu, H. Zhang, D. Ma, R. Wang, and P. Tu, "Small leak location for intelligent pipeline system via action-dependent heuristic dynamic programming," *IEEE Trans. Ind. Electron.*, vol. 69, no. 11, pp. 11723–11732, Nov. 2022.

[13] X. Han, W. Cao, X. Cui, Y. Gao, and F. Liu, "Plastic pipeline leak localization based on wavelet packet decomposition and higher order cumulants," *IEEE Trans. Instrum. Meas.*, vol. 71, pp. 1–11, Aug. 2022.

[14] X. Lang, P. Li, Y. Guo, J. Cao, and S. Lu, "A multiple Leaks' localization method in a pipeline based on change in the sound velocity," *IEEE Trans. Instrum. Meas.*, vol. 69, no. 7, pp. 5010–5017, Jul. 2020.

[15] Q. Meng, X. Lang, M. Lin, Z. Cai, H. Zheng, H. Song, and W. Liu, "Leak localization of gas pipeline based on the combination of EEMD and cross-spectrum analysis," *IEEE Trans. Instrum. Meas.*, vol. 71, pp. 1–9, Nov. 2022.

[16] S. Li, M. Cai, M. Han, and Z. Dai, "Noise reduction based on CEEMDAN-ICA and cross-spectral analysis for leak location in water-supply pipelines," *IEEE Sensors J.*, vol. 22, no. 13, pp. 13030–13042, Jul. 2022.

[17] C.-W. Liu, Y.-X. Li, Y.-K. Yan, J.-T. Fu, and Y.-Q. Zhang, "A new leak location method based on leakage acoustic waves for oil and gas pipelines," *J. Loss Prevention Process Industries*, vol. 35, pp. 236–246, May 2015.

[18] L. Sun, "Mathematical modeling of the flow in a pipeline with a leak," *Math. Comput. Simul.*, vol. 82, no. 11, pp. 2253–2267, Jul. 2012.

[19] J.-L. Wang and Z.-J. Li, "Extreme-point symmetric mode decomposition method for data analysis," *Adv. Adapt. Data Anal.*, vol. 5, no. 3, Aug. 2013, Art. no. 1350015.

[20] P. Xia, H. Xu, M. Lei, and Z. Ma, "An improved extreme-point symmetric mode decomposition method and its application to rolling bearing fault diagnosis," *J. Vibroengineering*, vol. 20, no. 8, pp. 2810–2824, Dec. 2018.

[21] Z. Zhang, L. Zhang, M. Fu, D. Ozevin, and H. Yuan, "Study on leak localization for buried gas pipelines based on an acoustic method," *Tunnelling Underground Space Technol.*, vol. 120, Feb. 2022, Art. no. 104247.

[22] X. Wang, L. Liu, R. Duan, Y. Liu, Z. Wei, X. Yang, X. Liu, and Z. Li, "A method for leak detection in buried pipelines based on soil heat and moisture," *Int. Commun. Heat Mass Transf.*, vol. 135, Jun. 2022, Art. no. 106123.

[23] C. Liu, Y. Li, L. Meng, W. Wang, and F. Zhang, "Study on leak-acoustics generation mechanism for natural gas pipelines," *J. Loss Prevention Process Industries*, vol. 32, pp. 174–181, Nov. 2014.

[24] X. Lang and Y. Zhu, "An analysis of detectable leakage rate for oil pipelines based on acoustic wave method," *Meas. Sci. Technol.*, vol. 33, no. 12, Dec. 2022, Art. no. 125108.

[25] A. Mostafapour and S. Davoodi, "A theoretical and experimental study on acoustic signals caused by leakage in buried gas-filled pipe," *Appl. Acoust.*, vol. 87, pp. 1–8, Jan. 2015.

[26] Y. He, D. Z. Zhu, T. Zhang, Y. Shao, and T. Yu, "Experimental observations on the initiation of sand-bed erosion by an upward water jet," *J. Hydraulic Eng.*, vol. 143, no. 7, Jul. 2017, Art. no. 06017007.

[27] J. M. Muggleton, M. Kalkowski, Y. Gao, and E. Rustighi, "A theoretical study of the fundamental torsional wave in buried pipes for pipeline condition assessment and monitoring," *J. Sound Vib.*, vol. 374, pp. 155–171, Jul. 2016.

[28] X. Liu, S. Li, and X. Tong, "Two-level W-ESMD denoising for dynamic deflection measurement of railway bridges by microwave interferometry," *IEEE J. Sel. Topics Appl. Earth Observ. Remote Sens.*, vol. 11, no. 12, pp. 4874–4883, Dec. 2018.

[29] X. Yu, J. Nichol, K. H. Lee, J. Li, and M. S. Wong, "Analysis of long-term aerosol optical properties combining AERONET sunphotometer and satellite-based observations in Hong Kong," *Remote Sens.*, vol. 14, no. 20, p. 5220, Oct. 2022.

[30] X. Liu, S. Zhao, and R. Wang, "ESMD-WSST high-frequency de-noising method for bridge dynamic deflection using GB-SAR," *Electronics*, vol. 12, no. 1, p. 54, Dec. 2022.

[31] X. Liu, M. Jiang, Z. Liu, and H. Wang, "A morphology filter-assisted extreme-point symmetric mode decomposition (MF-ESMD) denoising method for bridge dynamic deflection based on ground-based microwave interferometry," *Shock Vib.*, vol. 2020, pp. 1–13, Jun. 2020.

SONG LIU received the B.S. degree in environmental science from Sichuan University, Chengdu, Sichuan, China, in 2004, and the M.S. degree in environmental science from the China University of Mining and Technology, Beijing, China, in 2010.

Since 2004, he has been a Faculty Member with the College of Chemical Safety, North China Institute of Science and Technology. His current research interests include leakage detection, soil pollution monitoring, and ecological restoration.

ANQI LIU received the B.S. degree in geography information systems and the M.S. degree in resource planning and development from the China University of Mining and Technology, Beijing, China, in 2008 and 2011, respectively, and the Ph.D. degree in environmental chemical engineering from the China University of Petroleum (East China), Qingdao, Shandong, China.

Since 2011, she has been with the CNPC Research Institute of Safety and Environment Technology as a Research Team Leader. Her current research interests include leakage detection, environmental protection, and chemical process safety. She has published 18 journal articles in related fields.

ZEFENG CAI received the B.S. and M.B.A. degrees in transportation safety management from the Civil Aviation Flight University of China, Beijing, China, in 2014.

Since 2014, he has been with Beijing Haifurun Technology Company Ltd., where he is currently the Chief Technology Officer. He holds five patents in the area of leakage detection. His current research interests include leakage detection and transportation safety management.

CHUNFENG SUN received the B.S. and M.S. degrees in material science and engineering from Shandong University, Jinan, Shandong, China, in 2004.

Since 2004, he has been a Faculty Member with the College of Chemical Safety, North China Institute of Science and Technology. He has published 22 articles and four books. His current research interests include information systems, process safety, and fire protection materials.

RUOCHEN LIU received the B.S. degree in chemistry from Beijing Normal University, Beijing, China, in 2007, the M.S. degree in chemical engineering from Carnegie Mellon University, Pittsburgh, PA, USA, in 2011, and the Ph.D. degree in chemical engineering from the Mary Kay O'Connor Process Safety Center, Texas A&M University, College Station, TX, USA, in 2016.

From 2015 to 2016, he was a Consultant with DNV GL. From 2016 to 2018, he was a Process Safety Leader with the Wanhua Chemical Group. From 2018 to 2022, he was a Senior Consultant with DNV. Since 2022, he has been a Faculty Member and the Head of the Hebei Key Laboratory of Hazardous Chemicals Safety and Control Technology, College of Chemical Safety, North China Institute of Science and Technology. His current research interests include leakage monitoring and detection, risk assessment, and process safety management.